Spring 5-1-2012

Plasmonic Nanogel: Structure, Rheology, and Optical Properties

Georo Zhou

Plasmonic Nanogel: Structure, Rheology, and Optical Properties

A Capstone Project Submitted in Partial Fulfillment of the Requirements of the Renée Crown University Honors Program at Syracuse University

Georo Zhou
Candidate for B.S. Degree
and Renée Crown University Honors
May 2012

Honors Capstone Project in Chemical Engineering

Capstone Project Advisor: Professor Radhakrishna Sureshkumar

Capstone Project Reader: Professor Patrick T. Mather

Honors Director: Stephen Kuusisto

Date: April 25, 2012

Abstract

The invention of plasmonic nanogels (PNG) opens up the field of nanotechnology to a wide variety of applications such as, enhanced light trapping in solar cells, design of smart glasses, chemical detection, and optofluidic devices. In this work, it was determined that, the synthesis of a nanoparticle-micelle network in a fluid state is performed with the ability to suspend metal nanoparticles in a gel-like solution in a stable fashion. Furthermore, the stable suspension of the nanoparticles in the fluidic system allows the user to easily tune the PNG's optical and rheological properties by controlling the concentration of the nanoparticles and salts within the PNGs. Ultimately, the control of such properties enables the PNG to be used for many desirable applications.

Table of Contents

I. Acknowledgement

I would like to give a special thanks to Professor Radhakrishna Sureshkumar for giving me this opportunity to take part in his research group, for the guidance he provided on the research work, and for being an excellent honors capstone advisor. I would like to thanks Tao Cong, a graduate student, for allowing me to work with him on this research and for all the guidance he provided me on for my research experience. I would also like to give thanks to Professor Patrick Mather for being my honors capstone reader and providing good feedback on my capstone.

Advice to Future Students

Taking part in the honors program as an engineer is definitely a rewarding experience. As many of you would know, studying in engineering does not offer many chances to explore outside the bounds of the curriculum due to the immense difficulty of the field. However, should any of you decide to take on the challenge and experience fields outside of engineering, joining the honors program is one great way to get motivated. For example, I was able to take honors chemistry lab course, in which we spend a whole semester working on a research project to cure cancer. In addition, the global awareness requirement for the honors degree had motivated me to study abroad in a foreign country, which I considered as the best experience I had throughout my entire college life. Although many engineers feel like there is not enough time to accomplish both a B.S. in engineering and honors, truthfully this does not require a lot of additional work. I only had to take one additional course outside my major curriculum; everything else just takes good curriculum planning. Taking part in the honors program will definitely make your engineering education at Syracuse University much more enjoyable.

I. Introduction

The research in nanoparticles has been a growing field in recent years. Understanding the interaction of nanoparticles in complex systems would help designing many applications in medicine, energy harvesting, molecular detection, electronics, catalysis, and others. Metal nanoparticles have the ability to create localized surface plasmon resonance.[1] Such plasmonic nanoparticles could be used to tune the response of a material to electromagnetic spectrum in the ultraviolet (UV) to infrared range by varying the material, size or shape of the particles.[2] In this report, I will discuss the study of plasmonic nanogel (PNG) that consists of self-assembly of surfactant micelle with multicomponent nanoparticles with tunable optical properties.

Plasmons are the oscillations of free electron gas density waves. When light interacts with the surface of a metal, electron density waves are generated that have an optical frequency. Localized surface plasmon resonances can be utilized to confine electromagnetic fields to a small volume and varied by changing the shape and size of nanoparticles.[3] By confining electromagnetic fields to a small volume, a wide variety of wavelengths could be trapped within a small section of a device such as photovoltaic. As a result more light energy could be captured per unit surface area.

The great interest in metal nanoparticles, especially silver (Ag) and gold (Au), is their plasmonic ability, which could be utilized for potential applications in different fields including optical sensing, nanoscale waveguiding, plasmon enhanced solar cells, smart glass, optofluidic devices, and toxin detectors.

Although nanoparticles seem to be the key to many potent applications, the major difficulty of developing such application with the use of nanoparticles is because bare metal nanoparticles tend to agglormerate, when particles cluster together and binds to each other in normal solvent such as water, thus altering the shape and size of the particles. Furthermore, phase separation occurs between the nanoparticles and the solvent, which destroys unique optical property and functionality of the metal nanoparticles. To prevent the particles from agglomerating, nanoparticles are distributed in a network of worm-like micelles (WLMs) in this study.

Typical surfactant micelles are formed by the self-assembly of hydrophilic head group amphiphilic molecules, which each molecule has a hydrophilic head group and a hydrophobic tail group as shown in figure 1. When the surfactants are dissolved in an aqueous solvent at the critical micelle concentration (CMC), the surfactant molecules would self-assemble into a cluster with an interior consisting of hydrophobic tail groups and the head groups pointing towards the water phase. The versatility in the aggregation of micelles enables the formation of different structures such as spheres, rods, and WLMs depending on the concentration of surfactant, concentration of salt, and temperature of the solution.[4] At dilute concentrations, the surfactants aggregate into a spherical shape. As the concentration of surfactant increases, the spherical micelles elongate into rod-like micelles. With further increase in surfactant concentrations or with addition of counter-ionic salt, the rods will be able to grow to longer lengths up to several microns, which result in the formation of flexible “wormlike” micelles. In a

solution of sufficient concentration of surfactant and/or salt, WLMs will entangle to form a viscoelastic network that behaves like an entangled networks of strings, as shown in figure 2.

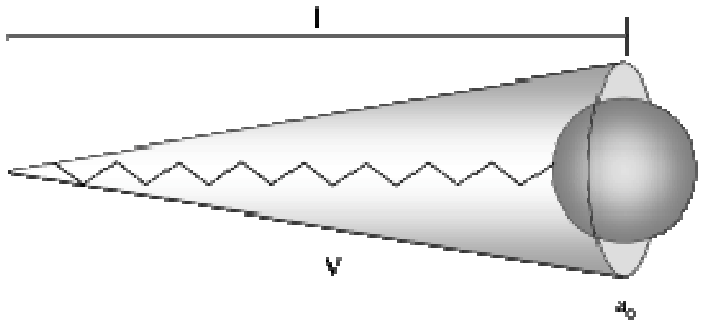

Figure 1. Illustration of a typical surfactant molecule including head group with projected area a_o and tail group with volume *V* and length *l*.[4]

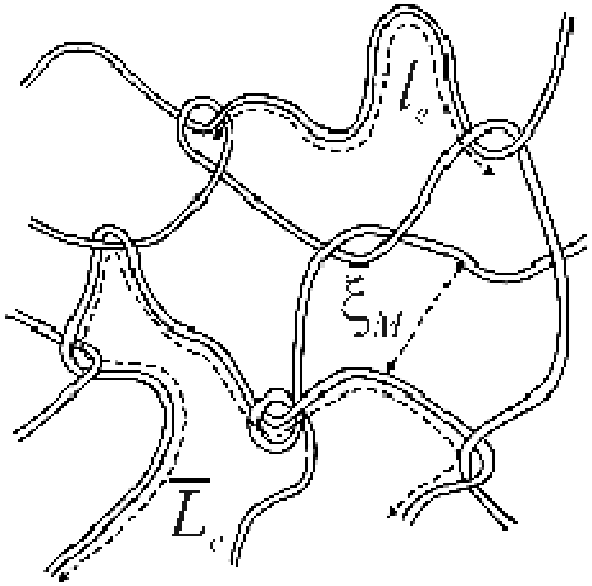

Figure 2. Illustration of an entangle micelles network and associated length scales.[4]

The characteristic lengths scales of the WLM network are the length of micelle strand ($\overline{L_c}$), the length between entanglements on a single strand (l_e), and the network mesh size (ξ_M). The length of a micelle strand is determined from the following Eqn. (1).

$$\overline{L_c} = l_e \frac{G_O}{G''_{\min}}, \tag{1}$$

where G_0 is the plateau of the storage modulus, $G''_{\min}$ is the local minimum of the loss modulus at high frequency, and l_e is the entanglement length estimated by

$$l_e = \frac{\xi_m^{5/3}}{l_p^{2/3}}, \tag{2}$$

where l_p is the persistence length of the micelle and the mesh size ξ_M is determined by the following Eqn (2).

$$\xi_m = \left(\frac{k_b T)}{G_O} \right)^{1/3}, \tag{3}$$

where k_b is Boltzmann constant and T is the absolute temperature.[4] When concentration of surfactant is increased beyond the minimum needed to form a WLMs network, l_e decreases due to the increase in number of entanglements forms. The addition of salt into the surfactant micelle solution will cause the WLMs to entangle more due to the increase in the ionic strength of the solution.

The WLMs network is able to create a stable suspension of nanoparticles at room temperature. Cetytrimethylammonium bromide (CTAB) surfactant and sodium salicylate (NaSal) or sodium nitrate ($NaNO_3$) salt were used to synthesize the wormlike micelle, since CTAB with salt is one of the most well studied system.[5] As suggested by Fourier transform infrared spectroscopy and

themogravimetric analysis[7] the CTAB surfactants are able to form a double layer structure around the surface of the nanoparticle as shown in figure 3.[7] The WLM could connect the interfaces between two nanoparticles through the endcap bridges.[8]

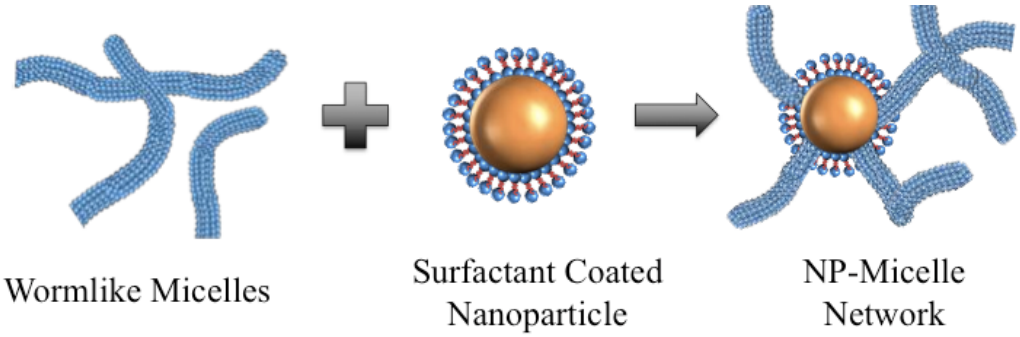

Figure 3. Simple illustration of self-assembly of WLMs with nanoparticles.[7]

The evidence of the formation of nanoparticle-micelle network can be obtained from rheological experiments and small angle x-ray scattering (SAXS). Figure 4 below shows analysis by using SAXS on the PNG consisting of 100 mM CTAB and different concentrations of Au nanoparticles.

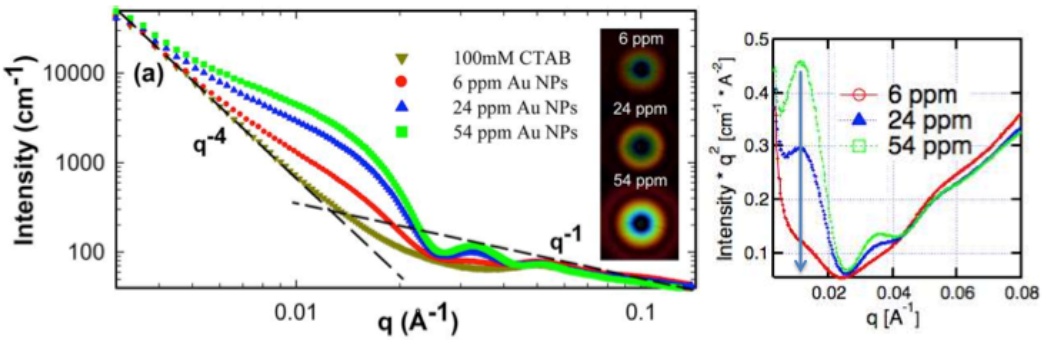

Figure 4. SAXS analysis of PNG of 100 mM CTAB and varying concentration of Au nanoparticles.[6,7]

The figure on the left shows a rapid decrease of intensity of q^{-4} at small q, which indicates that there is a sharp interface between the nanoparticles and

WLMs. This is followed by smaller decrease rate as q^{-1}, indicating that the gel-like substance is composed of cylindrical fibers. The sharp interface between the WLMs and nanoparticles indicates that junctions are formed between the nanoparticles and WLMs, while the cylindrical fibers are the strands in the network of WLMs.

The figure on the right shows a peak of the surfactant coated nanoparticle represented by the green line at q = 0.114 A^{-1}, which corresponds to the mean inter-particles distance of approximately 55.4 nm. This shows that the surfactant-coated nanoparticle is twice the diameter of the nanoparticles represented by the blue line.

In this study, we conducted optical and rheological measurements of PNG to support the formation of nanoparticle-micelle junctions and determine the PNG's flow behavior. The results are discussed in subsequent sections.

II. Results

A. Optical Properties - Single Nanoparticle Component PNG

The WLMs were prepared by vortex mixing CTAB and NaSal or $NaNO_3$ powder from Sigma-Aldrich with deionized (DI) water. The WLMs were then grown under 50 ^{o}C for 1 hour in an oven. Plasmonic nanogels (PNGs) were then made by the addition of nanoparticles with various shapes and sizes [i.e. Au nanoparticles (Nanopartz, Inc.) or silver Ag nanoparticles (Sigma-Aldrich)] to the WLMs solution while vortex mixing. All samples were then stored overnight at 24 ^{o}C under still condition for the sample to equilibrate.

The electromagnetic spectrum of the PNGs was measured using Ocean Optics USB 4000 UV-Visible spectrophotometer. Depending on the shape and size of the nanoparticles, the scattering and absorption of light vary significantly. In figure 5, the resonance peak red shifts from approximately 520 nm to 580 nm as the diameter of the gold nanospheres increases from 30 nm to 90 nm. Table 1 below, shows the resonance peak wavelength corresponding to the diameter size of the nanoparticles, respectively. For small nanoparticles absorption is the dominating extinction mechanism. On the other hand, for larger nanoparticles scattering is the dominating extinction mechanism. [9]

Gold Nanosphere	
Diameter (nm)	Wavelength (nm)
30	520
50	525
70	540
90	560

Table 1. Resonance peak wavelengths with corresponding nanoparticle diameter of gold nanosphere shown in figure 5.

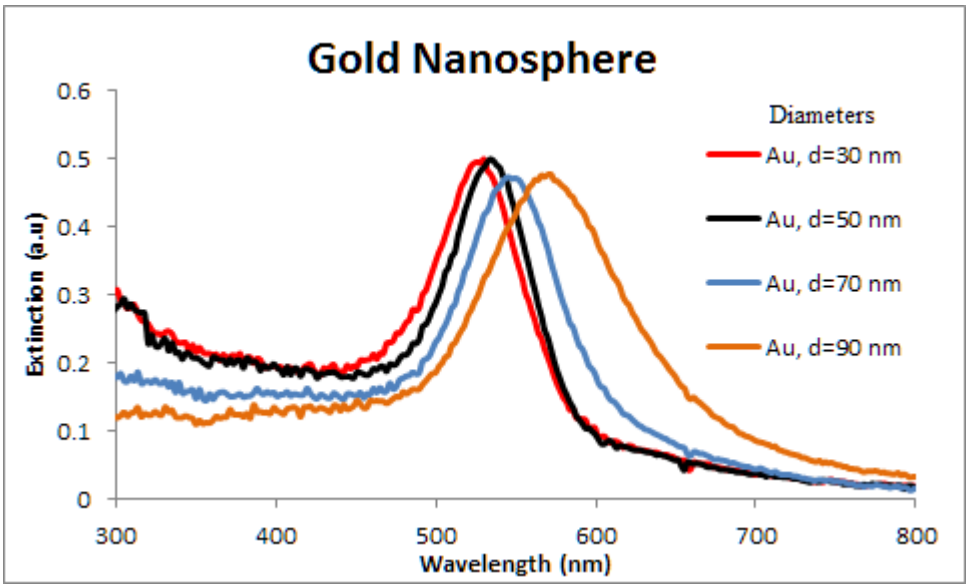

Figure 5. Samples of 30 nm, 50 nm, 70 nm, and 90 nm gold nanospheres disperse in WLM consisting of 100 mM CTAB and 30 mM $NaNO_3$.

The extinction cross-section of nanoparticles is determined from Eqn. (4):

$$\sigma_{ext} = \frac{18\pi\varepsilon_m^{\frac{3}{2}}V}{\lambda}\frac{\varepsilon_2(\lambda)}{(\varepsilon_1(\lambda)+2\varepsilon_m)^2+\varepsilon_2(\lambda)^2} \tag{4}$$

where, ε_m is the medium's dielectric function, V is the volume, λ is the wavelength, ε_1, and ε_2 are the real and imaginary components of dielectric functions of nanoparticle. Furthermore the scattering cross-section is determined by the following Eqn. (5):

$$\sigma_{sca} = \frac{32\pi^4\varepsilon_m^2V^2}{\lambda^4}\frac{(\varepsilon_1-\varepsilon_m)^2+(\varepsilon_2)^2}{(\varepsilon_1+2\varepsilon_m)^2+(\varepsilon_2)^2} \tag{5}$$

The difference of the extinction and scattering is the absorption cross-section of PNG. These equations operate under the assumption that the WLM solution does not affect the nanoparticle dielectric function. When $\varepsilon_1 = -2\varepsilon_m$ of the PNGs, then the extinction spectra approaches a maximum, which results in a sharp peak in the spectrum.[10]

In addition to nanospheres, nanoparticle can be created in various shapes, such as rods, cubes, prisms, stars, rices, etc. However unlike nanospheres, various shapes may increase the number of extinction peaks. For example, nanorods have two extinction peaks. One peak represents a plasmon resonance in the transverse (short axis) direction, while the other peak represents a plasmon resonance in the longitudinal (long axis) direction. The aspect ratio (*A*) of a nanorod corresponds to the ratio of the length of the longitudinal axis to the transverse axis diameter of the nanorod. Figure 6 below shows the resonance peaks of gold nanorods with varying aspect ratios. All nanorods have a transverse axis diameter of approximately 25 nm. Red shift occurs to the longitudinal extinction peak as the aspect ratio of the nanorod increases.

Gold Nanorods		
Aspect Ratio (A)	1st Wavelength (nm)	2nd Wavelength (nm)
1.4	540	540
1.8	540	590
2.3	540	640
3.0	540	680

Table 2. Resonances peaks wavelengths corresponding to the aspect ratio of gold nanorods shown in figure 6.

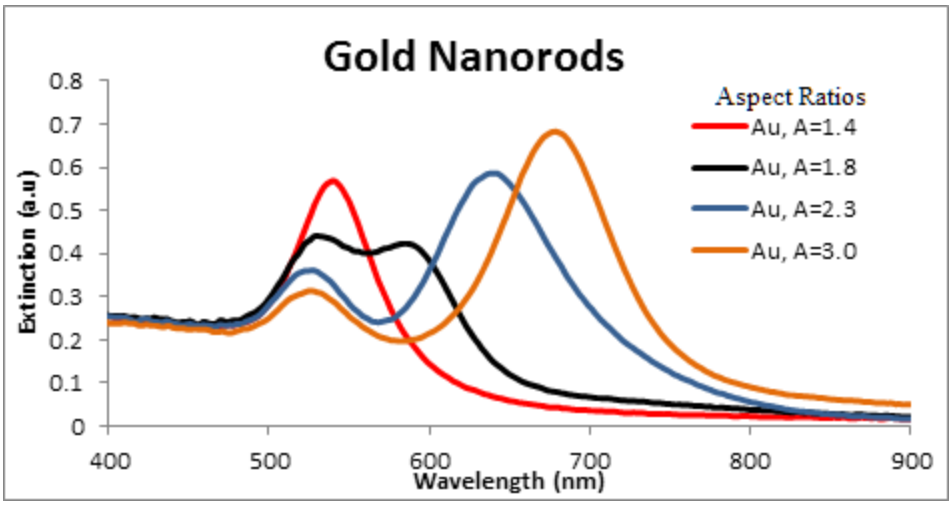

Figure 6. Extinction spectra of gold nanorods with diameter of ≈25nm and varying aspect ratios ranging from 1.4 to 3.0.

B. Optical Properties - Multiple Nanoparticles Components PNG

Depending on the size, shape, and material of the nanoparticles, different extinction spectra occur as discussed above. Under low concentrations of nanoparticles the extinction increases linearly with increasing concentration. As described previously, each type of nanoparticle exhibits distinct plasmonic spectra, such as 35 nm diameter of silver (Ag) nanosphere has a plasmon resonance peak at around 420 nm, 50 nm diameter of gold (Au) nanosphere has a plasmon resonance peak at around 520 nm, and A = 2.3 of Au nanorod has two plasmon resonance peaks at around 520 nm and 640 nm. Due to the distinct absorption of different type nanoparticle, the samples appear in a wide range of colors as shown in figure 7 below. Ag nanospheres, Au nanospheres, and Au nanorods exhibits in the primary colors of yellow, red, and blue respectively.

When multiple types of nanoparticles are used in combination, the resulting extinction spectrum is a superposition of the individual ones. For example, figure 8 shows the green PNG that is formed by the combination of Ag nanospheres (yellow) and Au nanorods (blue), exhibiting a spectrum with three plasmon resonance peaks corresponding to those of the individual nanoparticles at ≈420 nm, ≈520 nm, and ≈640 nm respectively.

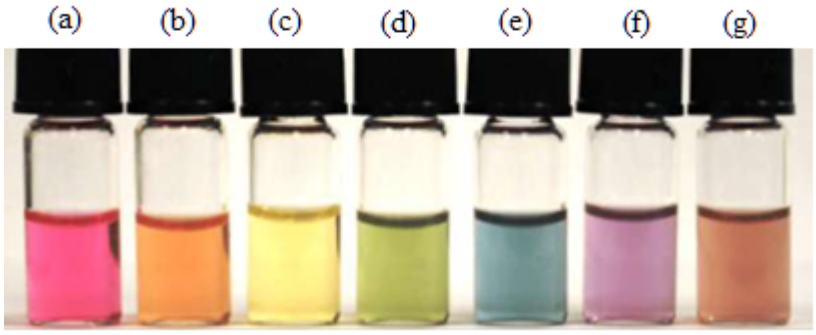

Figure 7. PNGs with various combinations of nanoparticles. The nanoparticles are suspended in a micelle network form with 100mM CTAB and 100mM $NaNO_3$ with various nanoparticle concentrations as follows: (a). red (20ppm of 50 nm Au nanospheres), (b). orange (10 ppm of Au nanospheres and 10 ppm of Ag nanospheres), (c). yellow (20ppm of 35nm Ag nanospheres), (d). green (10 ppm of Au nanorods and 25 ppm of Ag nanospheres), (e). blue (20 ppm of A = 2.3 Au nanorods), (f). purple (10ppm of Au nanospheres and 10ppm of nanorods), and (g). brown (5 ppm of Au nanospheres, 10 ppm of Au nanorods, and 15 ppm of Ag nanospheres).

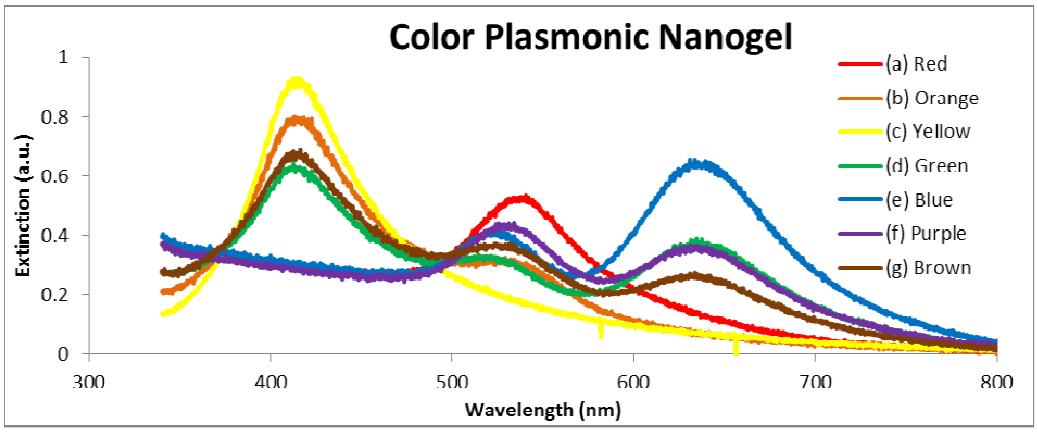

Figure 8. The extinction spectra corresponding to each sample shown in figure 7.

The ability to mix different nanoparticles into one PNG is the key to producing a broadband extinction spectrum that would cover a wide range of visible wavelengths. In figure 9 below, the combination of five different nanoparticles (35 nm Ag nanospheres, 70 nm Au nanospheres, A = 1.8 Au nanorods, A = 2.3 Au nanorods, and A = 3.5 Au nanorods) in 50 mM CTAB and 15 mM NaSal is used to create the PNG with broadband absorption.

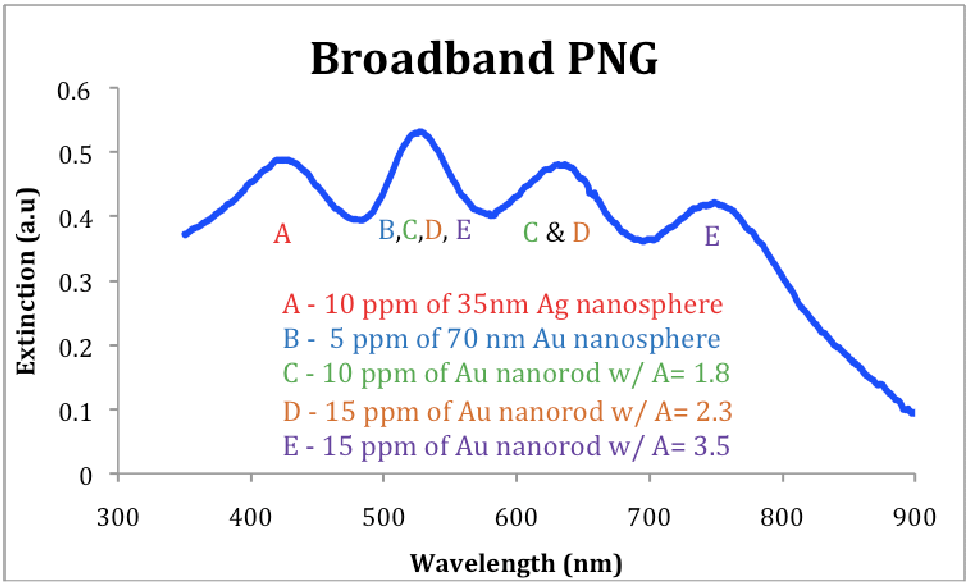

Figure 9. A PNG with five different types of nanoparticles exhibiting a relatively uniform extinction spectrum over the visible light region.

The spectrum spans the wavelengths in the entire visible light region, allowing the PNG to absorb more solar energy. The advantage of using the multicomponent nanoparticles enables the PNG to be tuned to absorb or scatter any desirable wavelengths for a wide variety of possible applications.

C. Rheology

PNGs possess tunable optical properties. In order to process the gels onto different substrates, the structural and flow behaviors of the gels need to be understood. We performed linear and nonlinear rheological experiments at room temperature using a TA Instrument AR-G2 rheometer with a cone and plate setup. The samples were prepared in the same method as in the optical section with the addition of carefully maintain the temperature of each at 25 ^{o}C to keep consistent data. By controlling the concentration of the surfactants, salts, and nanoparticles, PNGs exhibiting rich rheological behaviors including shear thickening, rheopexy, shear thinning, and viscoelasticity could be produced.

The addition of nanoparticles into WLMs solution greatly affects the rheological behavior of the solution. The samples shown in figure 10 were prepared with 50 mM CTAB and 10 mM NaSal for a ratio of 0.2 (R=0.2) of surfactant to salt concentrations. For the solution with no nanoparticles in the WLM solution, the sample shows Newtonian behavior within the shear rate ranging from 0.1 to 1000 s^{-1} (purple triangle). Newtonian behavior is when a fluid viscosity does not change with applying shear force (e.g. water). When nanoparticles are added to WLMs, the system forms a shear-induced structure

(SIS) under the flow. In the SIS regime, the viscosity increases as the shear rate is increased at low shear rates, suggesting the formation or build up of shear induced micelle-NP junctions. Under large deformation (high shear rate), such junctions tend to break leading to a decrease of the viscosity.

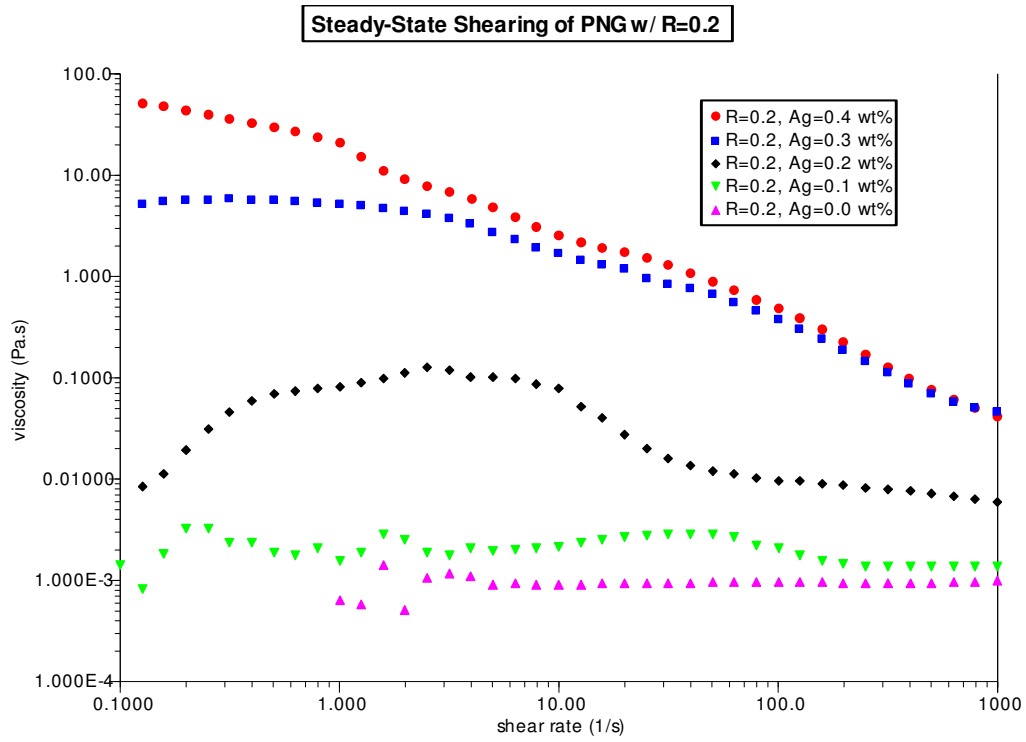

Figure 10. Viscosity of PNGs consisting of 50 mM CTAB and 10 mM NaSal [R=0.2] for different Ag nanoparticles concentration.

At higher nanoparticle concentrations (> 0.2 wt% Ag), it is hypothesize that the micelles could self-assemble with nanoparticles to form the double network in the absence of flow, as shown in figure 10 with the high initial viscosity when no shear is applied. In addition, at higher nanoparticle concentration, the critical shear rate shifts to the left resulting in the break up of the nanoparticle-micelle junctions at lower shear. For example, the sample with 0.3 wt% Ag shows a higher zero-shear viscosity than 0.2 wt% Ag sample and begins shear thins at a

lower critical shear rate. The decrease in viscosity implies the breakdown of the structure. In the case with the 0.4wt% nanoparticles sample (red circles), only shear thinning occurs, since the solution is saturated with nanoparticles to form a stable network with nanoparticle-micelle junctions.

To better understand the formation of SIS in PNGs with CTAB micelles, another set of PNGs with 15 mM NaSal to 50 mM CTAB [R = 0.3] was studied, as shown in figure 11 below. The sample with no nanoparticles (light blue square) shows shear thickening at a critical shear rate of 100 s^{-1}. However, with the addition of nanoparticles, SIS begins to form at lower critical shear rate as shown from for PNGs with 0.01 wt% to 0.1 wt% concentrations of silver nanoparticles. In addition to the shift of the critical shear rate, the viscosity increases as the concentration of nanoparticles increases, which indicates that more and/or complex nanoparticle-micelle junctions are forming. At 0.2 wt% the junctions in the PNG is saturated, thus only shear thinning was observed. Despite the difference in formation and breakage of SIS, as the shear rate increases to approximately 1000 s^{-1} the viscosity of all the samples converges; this indicates that at high shear rate, all nanoparticles-micelles junctions break and all entanglement of the WLMs separates. Thus, no matter the concentration of nanoparticle the viscosity of the PNGs is the same under intense shear.

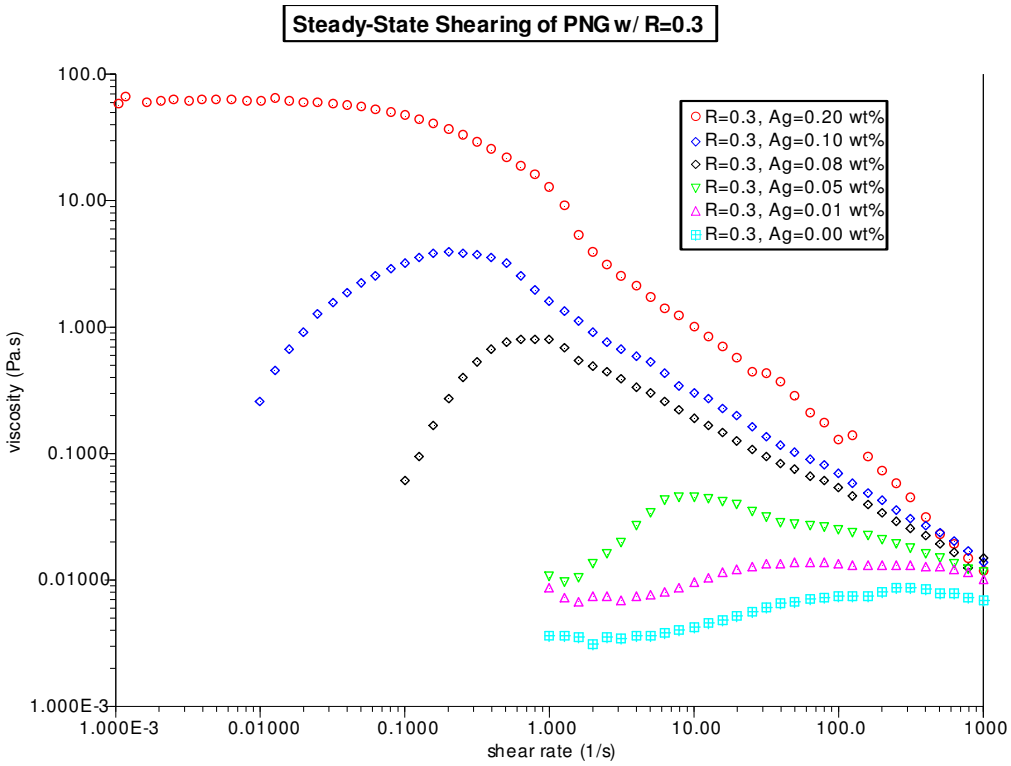

Figure 11. Viscosity of 15 mM NaSal to 50 mM CTAB [R = 0.3] for different Ag nanoparticles concentrations.

Further study of the formation of SIS shows that under low concentration of silver nanoparticles, the PNG follows a rheopectic behavior. Rheopectic behavior is characterized by an increase in the viscosity of the sample with time, while being sheared at a constant shear rate. When the viscosity of a sample reaches a plateau, while being shear under constant shear rate, it indicates that the sample has abstained a time-independent state. As shown in figure 12 below, PNG under a higher shear-rate has a lower plateau viscosity, indicating that the structure is prone to breaking. In addition to having a lower plateau at higher shear rates, the time to reach the plateau or relatively little to no increase in viscosity decreases as shear rate increases; this indicates that at higher shear rate the sample reaches its steady state in shorter time interval. A shallow maximum

viscosity is shown for the shear rate of $1s^{-1}$. This indicates the saturation of SIS and the possibility that the PNG might undergo flow alignment of the micelle-nanoparticle network.

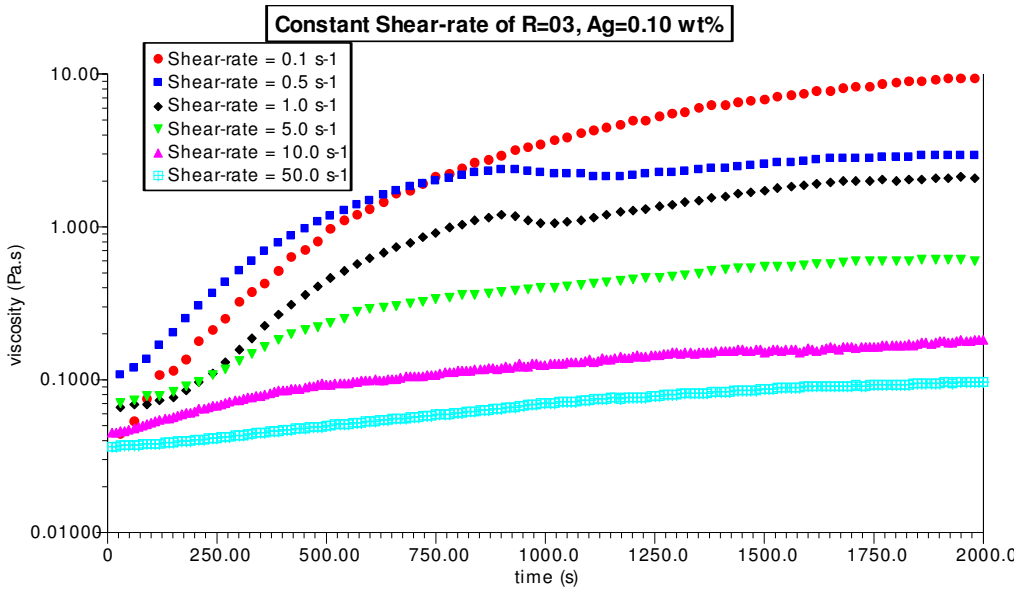

Figure 12. Viscosity vs. time for 0.1 wt% Ag nanoparticles in 15 mM NaSal and 50mM CTAB [R = 0.3] at different shear rates.

PNGs with different types of salt and different concentrations of CTAB exhibit various rheological behaviors. For example, the analysis of the shear-thinning region of the PNG under steady state shearing of 100 mM CTAB/100 mM Sodium Nitrate ($NaNO_3$) is shown in figure 13. After the sample was pre-sheared at a very low shear rate, a steady shear experiment was performed with increasing shear rate. The increase of zero shear viscosity, μ_0 from 0.04 to 2.47 Pa•s as concentration of the nanoparticles in the PNG increased from 0.00 to 0.20 wt% is consistent with the formation of nanoparticle-micelle junctions. As shown in figure 13, the shear thinning of PNG can be fitted by Carreau Model, which is described by Eqn. 6,

$$\mu = \mu_{\infty} + \mu_{o} - \mu_{\infty}(l + \lambda\dot{\gamma}^{2})^{n-12} \tag{6}$$

where μ is the viscosity, $\dot{\gamma}$ is the shear-rate, μ_0 is the initial viscosity, μ_∞ is the infinity viscosity, *l*, and *n* are material parameters.

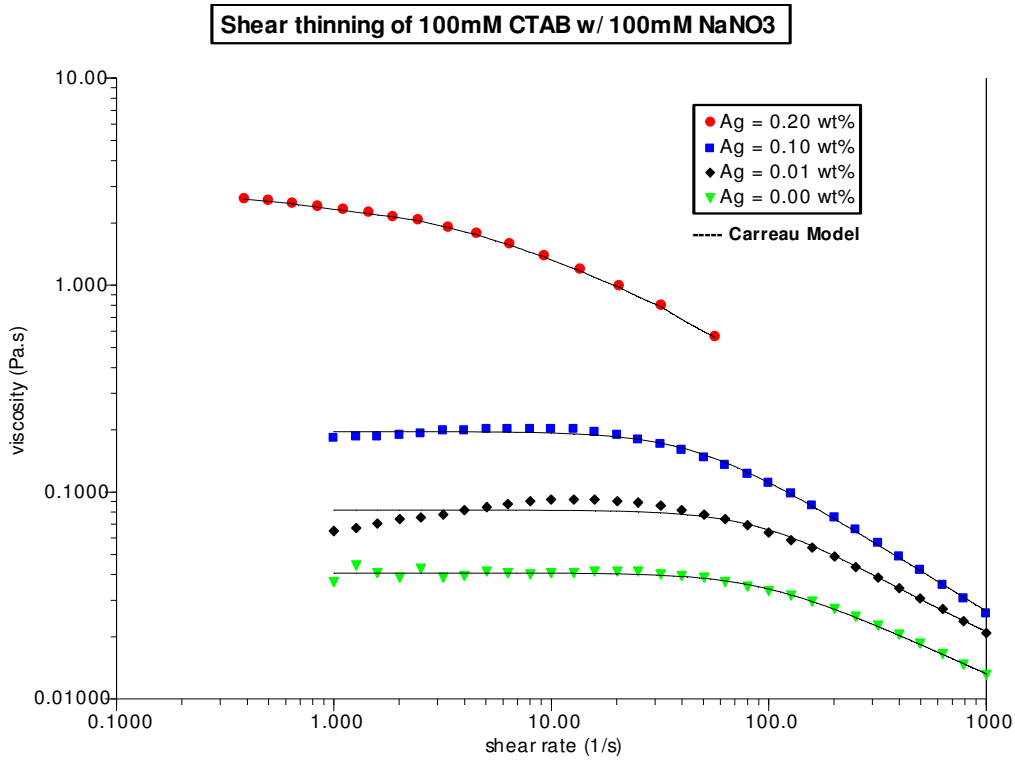

Figure 13. Viscosity of PNG with 100 mM CTAB with 100 mM $NaNO_3$ with varying silver nanoparticle concentrations.

Another data set supporting the formation of nanoparticle-micelle junction is shown in figure 14. The increase of plateau storage modulus (G_0) as concentration of silver nanoparticles is increased from 0.01 wt% (purple) to 0.20 wt% (red) indicates an increase in network density (r_{net}) of the PNGs, which is determined by Eqn. 7,

$$r_{net} = (\xi_M)^{-3} \tag{7}$$

where, ξ_M is the mesh size that was previously determined by Eqn. 3. The increase in network density is another evidence for the formation of nanoparticle micelle junctions.

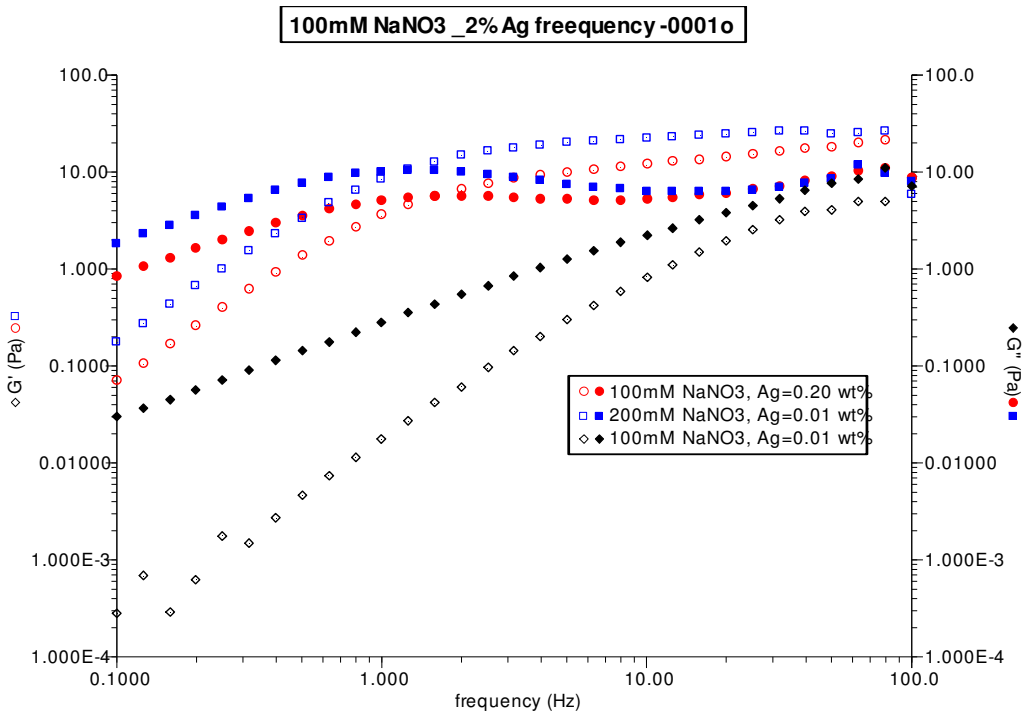

Figure 14. Storage modulus, G' (open symbol) and Loss modulus (closed symbol) of PNGs. 100 mM CTAB with 100 mM $NaNO_3$ and 0.20 wt% Ag nanoparticles (circles). 100 mM CTAB with 200 mM $NaNO_3$ and 0.01 wt% (squares). 100 mM CTAB with 100 mM $NaNO_3$ 0.01 wt% Ag nanoparticles (diamonds).

III. Possible Applications and Future Work

The ability to tune the composition of multi-component PNGs to absorb various wavelengths of light opens up the possibility to design a wide variety of optical devices. Furthermore, the study of the rheological behaviors of the PNG shows that under stress, the PNG is able to change its flow behavior, which is useful information for designing optofluidic applications for PNGs.

The self-assembly of nanoparticles in WLMs to create PNG with tunable optical and the rheological properties provides an opportunity to create and design optofluidic systems. Optofluidic systems contain fluids that have unique properties that cannot be found in solids and have the ability to alter optical response by application of mechanical or electrical stimulus, such as the absorption or reflection of certain wavelengths of light.[11] Advantages of optofluidic systems are that they can be more easily replaced or reconfigured by adjustment of flow rates and the various possible uses due to being in a readily moveable form. Possible uses of optofluids are flows through dual pane glass, coating for solar cells, chemical detection surfaces, and smart glass.

Current solar panels are inadequate due to high cost of material and installation as well as low efficiencies. Around 40 % of the cost of a silicon (Si) solar cell arises from the cost of the silicon wafer. Thin-film solar cells have the potential to make a large contribution to cost reduction, since this approach makes it possible to significantly reduce the amount of the semiconductor material used in the finished product. However, the efficiencies of such thin film solar cells with thickness in several micrometer ranges are much lower than those of the

conventional wafer-based cells because of poor light collection. One potential use of the PNGs is for coating on thin solar cells to enhance light trapping. The PNGs can be used as a feedstock for impacting a desired optical property to a substrate or interface, e.g. via dip coating, spin coating, or spraying, followed by solvent evaporation. As shown previously, multi-component PNGs have the ability to absorb/scatter a broad band of visible light wavelengths. This ability would allow the PNG coating on solar cell to capture and convert more solar energy into electricity.

Another possible design of PNGs is for coating on glasses for the development of smart glass. PNGs designed for smart glass would be tuned differently for each special function of the smart glass. For example, PNGs could be coated on windows with self-adjustment properties for heating in a house. PNGs could be tuned to reflect or absorb more light during summer times to prevent or limit solar heat from passing through the window, while during winter times the PNG would be adjusted to allow more solar heat to transmit through the windows. Another potential use of the smart glass with PNGs is chemical detection. Since, metallic nanoparticles are capable of reacting with a variety of chemicals, glass coated with PNG could be tuned to detect a certain airborne contaminant by changing colors.

Besides coating for glass and solar cells, optofluids could be used in dual-pane windows as a flow system. Similar to smart glass with PNG tuned to reflect or transmit light depending on the temperature, using a dual-pane window could create a flow system for PNG, in which the optical properties could adjusted by

changing the flow rate and in the system. In addition to temperature dependence, the dual-pane window can be used as a home design display with self-adjusting light by simply changing the flow rate of the PNG across the window.

Since the study of nanoparticles and PNG are relatively new technologies, further research into these topics is needed before it can be implemented into real world applications. Future research needs to address effective procedures for coating PNG onto glass and solar cells, the relation of optical properties as function of flow rate, simulations of nanoscopic interaction in PNG, and nanoparticle dispersion in other medium (e.g. block copolymers).

IV. Conclusion

The self-assembly of nanoparticles in WLMs to create PNGs open up opportunities for the development for a wide variety of applications. Originally, nanoparticles in solution (e.g. water) tend to agglomerate and separate into different phases. In our research we were able to synthesize plasmonic nanogels capable of suspending nanoparticles in a stable network by self-assemble nanoparticles with WLMs. The optical properties of the PNG can be easily tuned by the varying concentrations of the multiple nanoparticle species used. In addition to the robustly tunable optical properties, the rheological properties of PNGs could be controlled by varying the concentrations of surfactant, salt, and nanoparticles. The low viscosity of multi-component PNGs at room temperature makes it an ideal fluid for optofluidic systems. PNGs could be a key platform for innovation in many areas of technology including solar cell enhancement, photovoltaic devices, smart building envelopes, optoelectronics, and chemical detection system.

V. Summary for Non-Expert Readers

The invention of plasmonic nanogels (PNG) opens up a wide variety of applications such as, enhanced solar cells, smart glass designs, chemical detection devices, optofluidic devices, and optoelectronics. In this work, a nanoparticle-micelle network is synthesized in a fluid state with the ability to suspend metal nanoparticles in a gel-like solution. The stable suspension of the nanoparticles in the fluidic system allows the user to tune the PNG optical and rheological properties by simply controlling the concentrations of the nanoparticles and salts within the PNGs. Ultimately, the control of such properties enables the PNG to be used for many desirable applications.

Plasmonic nanogels are a fluidic gel-like solution containing metal nanoparticles and surfactant micelles that exhibits of localized surface plasmon resonance (LSPR). LSPR is the oscillation of the electron charged density in metal nanoparticles. LSPR is the result of light hitting a nanoparticle and exciting the electrons to oscillate in a thin plasmonic field between the metal surface and the surrounding medium. The significance of LSPR is that it is able enhance the surface absorption and scattering of certain wavelengths of light.

Typically, metal nanoparticles tends to agglomerate in normal solution, such as water. Agglomeration is when particles clusters and stick together forming larger particles. This occurs for nanoparticles in solutions like water due to the density of metal nanoparticles being greater than water; as a result, the nanoparticles will sink to the bottom over time, where they are able to cluster together, thus resulting in a nanoparticle to solvent layer separation and

agglomeration of nanoparticles. In order to prevent this from occurring, the nanoparticles are suspended in a solution of surfactant worm-like micelles.

Surfactants are usually organic compound with a hydrophilic head group connected to a hydrophobic tail group. Thus in water, the surfactant micelles are able to self-assemble together with interlocking tail groups in the center and the head groups forming a barrier layer between the tail groups and water. At sufficient concentration and temperature, the micelles are able to elongate and form a "wormlike" strand of surfactants known as worm-like micelle (WLM). With multiple WLMs in a solution, the WLMs will entangle with each other to create a viscoelastic network.

When metal nanoparticles are introduced into the WLM solution, the surfactants would encompass around each particle forming a double layer structure of nanoparticle and surfactant. The coating of surfactant around the nanoparticle allows the nanoparticle to interact and form additional junction in the micelle network. As a result, the nanoparticles can be suspended throughout the solution, thus preventing agglomeration and layer separation from occurring.

Small angle x-ray scattering SAXS data analysis suggests a direct link between the nanoparticles and WLMs. In addition, the data indicates that the solution is a gel-like substance that is composed of cylindrical fibers. The link between the WLMs and nanoparticles suggests that junctions are form between the nanoparticles and WLMs, while the cylindrical fibers are the strands in network of WLMs. Furthermore SAXS data analysis shows that three structures thickness are presented in the solution. The three structures correspond to the

WLM, the nanoparticle, and the double layer structure of surfactant-coated nanoparticle.

Rheology data analysis suggests that with the increase in the concentrations of surfactant and salt, viscosity of the solution would increase, thus making the solution more gel-like. With the addition of nanoparticles into the solution, the initial viscosity of the solution would increase even more. The increase of the viscosity suggests the formation of shear-induced structures (SIS), which is the build up of entanglement and junctions in solution. Further study into SIS, suggests the formation is a rheopectic behavior, in which the increase in viscosity is not only shear-rate dependant, but time dependant too. When solution viscosity attain a plateau, that indicates that the solution is saturated with junctions and that no more SISs are able to form. Under steady-state shearing, when the solution reaches its critical shear rate, the SIS breaks down and shearing thinning occurs leading to a break up of all structures in the solution.

In addition to flow testing of the solution, oscillation testing shows the plateau of the storage modulus, G', increases as nanoparticle concentrations increase, thus indicating an increase of the network density. Furthermore, not only the increase in nanoparticles increases network density, but the addition of salt will increases the network density too. An increase in network density indicates that more junctions or entanglement of the WLMs occurs.

One major motivation to use of metal nanoparticles is because of the plasmonic properties they have to enhance the absorption and scattering of light. Since nanoparticles can be synthesized with different materials, shape and sizes,

each nanoparticle has a distinct optical property. For example, 30 nm in diameter gold (Au) nanospheres exhibits an extinction peak at a light wavelength of 520nm. Unlike Au nanosphere, Au nanorod exhibits two extinction peaks, since it has two unequal length directions for the excited electron density to resonate.

With the use of WLMs network to suspend nanoparticles, multiple nanoparticles components could be used for a single PNG. For example, a combination of the gold nanospheres, gold nanorods, and silver nanospheres any possible colors of PNG can be synthesized, since the three nanoparticle manifest in the three primary color of red, blue, and yellow respectively. The uniform color of combine PNGs indicates that the nanoparticles were uniformly dispersed throughout the solution. Optical spectroscopy analysis of the color samples shows that extinction peaks occurs at only three general wavelengths corresponding to the three types of nanoparticles. These samples are evidence that shows that the nanoparticles are uniformly dispersed and suspended through the PNG.

PNGs optical properties are easily tuned to almost any desirable optical spectrum by varying the concentration of different nanoparticles. For example, using five different types of nanoparticles in one PNG creates a broad absorption peak that spans across the entire visible light regime. The significance of this PNG is that it could use as a possible thin film coating for solar cells, in order to enhance its efficiency by trapping more light energy of a wide range of wavelength. In addition, to enhancing solar cells efficiency, PNGs could be use for developing smart glass technology, optofluidic devices, optoelectronics, photovoltaic devices, and many more.

PNGs open the opportunity for the development of numerous applications with nanoparticles because of its nanoparticle suspension capability. PNGs' optical properties and rheological are easily tunable to absorb, scatter, or reflect a wide range of wavelength of light the development of PNG for many optical devices and fluidic devices by adjusting the concentration of surfactants, salt, and nanoparticles. Furthermore, PNG are simple to synthesize, since that surfactant coated nanoparticle and the WLMs network are able to self-assemble in the solution. Plasmonic nanogel could be a key factor in igniting a new branch of optical technology.

VI. Work Cited

1 - S. A. Maier, and H. A. Atwater, "Plasmonics: Localization and guiding of electromagnetic energy in metal/dielectric structures," Journal of Applied Physics, 98, 011101 (2005).

2 - Tao Cong, Satvik N. Wani, Georo Zhou, Elia Baszczuk and Radhakrishna Sureshkumar, "Plasmonic nanogels with robustly tunable optical properties", Proc. SPIE 8097, 80970L (2011); doi:10.1117/12.894070

3 – W.A. Murray, W.L. Barnes. “Plasmonic Materials”. Advanced Materials. p. 3771-3782. (2007). DOI: 10.1002/adma.200700678

4 – M. E. Helgeson, “Structure, Rheology, and Thermodynamics of Wormlike Micelle-Nanoparticles Mixtures” (2009)

5 - G. Hertel, and H. Hoffmann, “Lyotropic nematic phases of double chain surfactants,” Trends in Colloid and Interface Science II, 123-131 (1988)

6 – Tao Cong, et al. "Structure and optical properties of self-assembled multicomponent plasmonic nanogels." Applied physics letters 99.4 (2011)

7- T. Cong, S. Wani, G. Zhou, E. Baszczuk, A. Sambasivam, A. Sangwai, and R. Sureshkumar. “Plasmonic Nanogels With Tunable Optical Properties”. 83rd Annual Society of Rheology Poster Competeion. (2011)

8 - B. Nikoobakht, and M. A. El-Sayed, “Evidence for bilayer assembly of cationic surfactants on the surface of gold nanorods,” Langmuir, 17(20), 6368-6374 (2001)

9 - Jodar-Reyes, A B, and F. A. M.Leermakers. "Can Linear Micelles Bridge between Two Surfaces." The Journal of Physical Chemistry. B 110.37 (2006):18415-18423.

10 - Bohren, C. F., and Huffman, D. R., “Absorption and scattering of light by small particles,” Research supported by the University of Arizona and Institute of Occupational and Environmental Health. New York, Wiley-Interscience, 1983, 541 p., 1, (1983).

11 - Kathryn, M M, and H H HJason. "Localized Surface Plasmon Resonance Sensors." Chemical reviews 111.6 (2011):3828.

12 - Psaltis, D., Quake, S. R., and Yang, C., “Developing optofluidic technology through the fusion of microfluidics and optics,” Nature, 442(7101), 381-386 (2006).